ResearchGate

See discussions, stats, and author profiles for this publication at: https://www.researchgate.net/publication/331309175

# Subdividing the tectonic elements of Aegean and Eastern Mediterranean with gravity and GPS data

**Article** *in* Acta Geophysica · February 2019

DOI: 10.1007/s11600-019-00270-w

CITATIONS
7

READS
683

**5 authors**, including:



Muzaffer Kahveci
Paksoy Teknik Hizmetler, Ankara, Turkey
**19** PUBLICATIONS **61** CITATIONS
SEE PROFILE



Ayça Yurdakul Çırmık
Dokuz Eylul University
**39** PUBLICATIONS **143** CITATIONS
SEE PROFILE



Fikret Dogru
Ataturk University
**46** PUBLICATIONS **46** CITATIONS
SEE PROFILE



Oya Ankaya Pamukçu
Dokuz Eylul University
**101** PUBLICATIONS **468** CITATIONS
SEE PROFILE

**Some of the authors of this publication are also working on these related projects:**



EXAMINATION OF GEODYNAMIC STRUCTURE OF GULBAHCE FAULT AND ITS SURROUNDINGS View project



personal interest View project

All content following this page was uploaded by Ayça Yurdakul Çırmık on 25 February 2019.

The user has requested enhancement of the downloaded file.

Acta Geophysica
https://doi.org/10.1007/s11600-019-00270-w

RESEARCH ARTICLE - SOLID EARTH SCIENCES

# Subdividing the tectonic elements of Aegean and Eastern Mediterranean with gravity and GPS data

**Muzaffer Kahveci[1] · Ayça Çırmık[2] · Fikret Doğru[3] · Oya Pamukçu[2] · Tolga Gönenç[2]**

Received: 30 October 2018 / Accepted: 11 February 2019
© Institute of Geophysics, Polish Academy of Sciences & Polish Academy of Sciences 2019

**Abstract**
Western Anatolia has been formed by the motions of the African plate, Arabian plate and Hellenic Subduction zone. The Hellenic Subduction zone, which has high seismicity, is the main tectonic feature of the eastern Mediterranean Sea related to the subduction of the African Plate beneath the Aegean Sea Plate. The Hellenic Subduction zone has a complex lithospheric structure and shows complex differences in the Aegean Sea in terms of continental crust thickness and mantle velocity. In the study area, the directions of Global Positioning System (GPS) velocity vectors which are towards SE change towards S from North of Western Anatolia to Hellenic Subduction zone. It is thought that the factor which controls this mechanism is the shear force or subduction zone located in Aegean Sea. Western Anatolia region, which is located in Western Anatolia Extensional province, includes several morphologically significant N–S trending active normal faults. Besides, the NE–SW and NW–SE trending faults, which their kinematic features change from north to south, are very effective on the tectonic regime of the region. Additionally, for determining the boundaries of these tectonic elements, the Complete Spherical Bouguer (CSB) gravity anomaly of study area was calculated by using World Gravity Map (WGM2012) model. Moreover, in historical and instrumental studies, the high seismicity of the study area is remarkable. It is thought that this case is also related with the mechanism which oriented the GPS velocity vectors to southward. Consequently, the dominant kinematic structure of the region was classified by combining the GPS velocity vectors computed for Izmir and its surroundings bounded by Western Anatolia, Aegean Sea and Eastern Mediterranean and the CSB gravity anomaly. Finally, the results were interpreted together with focal depth distributions of earthquakes and Bouguer gravity data.

**Keywords** GPS · Tectonic elements · WGM2012 model · Gravity · Western Anatolia · Eastern Mediterranean · Aegean Sea

## Introduction

The tectonic movements of Arabian, African and Eurasian plates have formed the Eastern Mediterranean tectonism by compression in Eastern Anatolia, extension in Western Anatolia and faulting along North Anatolian Fault and East Anatolian Fault zones. Therefore, the Anatolian block has moved to W–SW, and additionally, due to the movement of African plate towards Eurasian plate, these oceanic subductions are driven throughout Hellenic Subduction zone (Fig. 1) (McKenzie 1972; Le Pichon and Angelier 1979; McClusky et al. 2000; Mart and Ryan 2003; Pamukçu 2016). The roll-back system of the Mediterranean slab subduction under the Aegean Sea causes the great subduction throughout Hellenic Subduction zone. Additionally, the slab pull force in the Mediterranean creates N–S extension in the Western Anatolia and Aegean region (Le Pichon and Angelier 1979; Le Pichon 1982; Mercier et al. 1989; Sorel et al. 1988).

The Western Anatolia is one of the most active extensional regions in the world (McKenzie 1978; Le Pichon and Angelier 1979; Dewey et al. 1986; Jackson and McKenzie 1988; Taymaz et al. 1990; Ambraseys and Jackson 1990; Goldsworthy et al. 2002; Nyst and Thatcher 2004). For clarifying the reason of extension, different models were suggested by Dewey (1988), Seyitoğlu and Scott (1991),

✉ Ayça Çırmık
ayca.cirmik@deu.edu.tr

[1] Department of Geomatics Engineering, Engineering and Natural Sciences Faculty, Konya Technical University, Konya, Turkey

[2] Department of Geophysical Engineering, Engineering Faculty, Dokuz Eylul University, Buca, Izmir, Turkey

[3] Department of Geophysical Engineering, Oltu Earth Sciences Faculty, Atatürk University, Oltu, Erzurum, Turkey

Published online: 23 February 2019

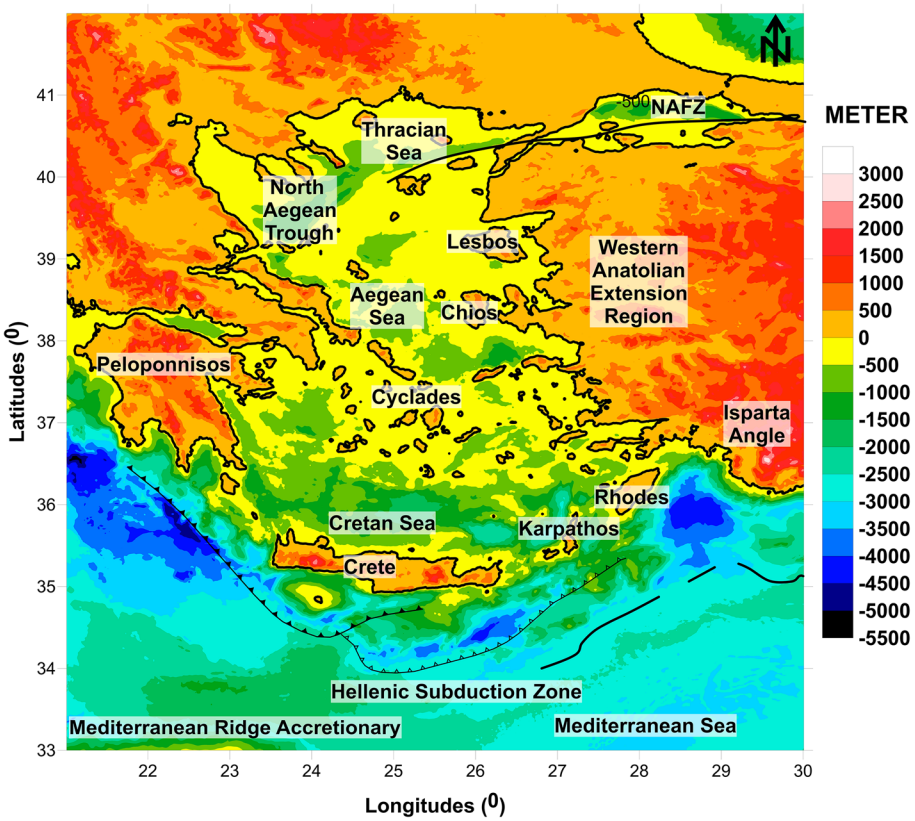


**Fig. 1** The main tectonic structures in the study area (Gessner et al. 2013, the topographic data were obtained from TOPEX; Smith and Sandwell 1997)

Dewey and Şengör (1979) and Le Pichon and Angelier (1979). These models were presented as four type models: the first is Anatolian plate escape, the second is orogenic collapse, the third is back-arc extension, and the last one is the combined model of the three models. In According to Yılmaz et al. (2000)and Bozkurt and Sözbilir (2004) the N-S trending extensional system of Western Anatolia has been still active since Mio-Pliocene.

Reilinger et al. (2010) pointed out that there was no coherency between the recent motions of the Aegean region and the previous geophysical and geological findings of previous studies (Makris 1978; Armijo et al. 1996). The GPS studies were carried out in Aegean region (McClusky et al. 2000; Kahle et al. 2000; Reilinger et al. 2006, 2010) indicating that the southward of Aegean Sea and Peloponnisos transform towards SW with minor internal deformation and according to Reilinger et al. (2010) new fault system causes these transformations.

Western Anatolia and Aegean Sea, which are chosen as the study region in this study, were evaluated in the previous studies (McClusky et al. 2000; Reilinger et al. 2006; Nyst and Thatcher 2004; Floyd et al. 2010) as blocks due to the relative motions. In the study of Nyst and Thatcher (2004), it was indicated that the GPS velocity vectors in and around Izmir were distinct from Western Anatolia. Hence, GPS measurements were carried out in 2009, 2010, 2011 for observing the behaviours of main tectonic structures located in Izmir and its surroundings by Kahveci et al. (2013), Pamukçu et al. (2015) and Çırmık et al. (2017).

In this study, the Eurasia-fixed-frame solutions of McClusky et al. (2000), Hollenstein et al. (2008), Çırmık et al. (2017) and Çırmık and Pamukçu (2017) were evaluated together and consequently, new microplate models were proposed for Western Anatolian region, Aegean Sea and eastward of Hellenic Subduction zone by examining the Eurasia-fixed-frame solutions with Complete Spherical Bouguer (CSB) gravity anomalies, earthquake focal depth distributions. In this study, the study region was divided into seven microplates and three regions due to the differences on the amplitudes and directions of GPS velocities, topographic/bathymetric and CSB gravity anomaly values. Additionally, when seismicity, gravity anomaly values and the microplate borders were evaluated it was found that the transitions in low and high seismicity zones present the borders of the microplates; therefore, it can be said that the separation of the study area into microplates was related with the density changes in the tectonic elements.

The whole steps of the study are given briefly with a flow-chart for following the applications clearly.

## Analysis of the GPS solutions

In the scope of this study, the GPS velocities of four different studies (McClusky et al. 2000; Hollenstein et al. 2008; Çırmık et al. 2017; Çırmık and Pamukçu 2017) were evaluated together for examining the velocity change related with the kinematic structure in Western Anatolia, Aegean Sea and Eastern Mediterranean (Fig. 2). The GPS data of McClusky et al. (2000) and Hollenstein et al. (2008) belong to the years between 1988–1997 and 1993–2003, respectively. The GPS data of Çırmık et al. (2017) and Çırmık and Pamukçu (2017) belong to 2009, 2010 and 2011.

Before evaluating all GPS velocities, a reference frame transformation is needed since the GPS velocities of McClusky et al. (2000) were calculated with ITRF96, Hollenstein et al. (2008) were calculated with ITRF00 and the GPS velocities of Çırmık et al. (2017) and Çırmık and Pamukçu (2017) were calculated with ITRF08. By calculating the rotation between common sites of two velocity fields, the reference frame effect was removed. In this study, ITRF08 was chosen as the reference frame and the frames of McClusky et al. (2000) and Hollenstein et al. (2008) were transformed to ITRF08. Initially, the GPS data of Çırmık et al. (2017) and Çırmık and Pamukçu (2017) were processed together with ITRF08 with Gamit/Globk (Herring et al. 2015) software. During processing, for increasing the common sites with McClusky et al. (2000) four IGS stations (NYAL, KIT3, METS, JOZE) were added. In this way, by calculating the rotation between Çırmık et al. (2017), Çırmık and Pamukçu (2017) and McClusky et al. (2000) at six common sites (KRPT, WTZR, NYAL, KIT3, METS and JOZE) and between Hollenstein et al. (2008) at nine common sites (KRPT, BUCU, GLSV, ISTA, MATE, NICO, TUBI, WTZR and ZECK), the reference frames effects were removed by using Gamit/Globk software.

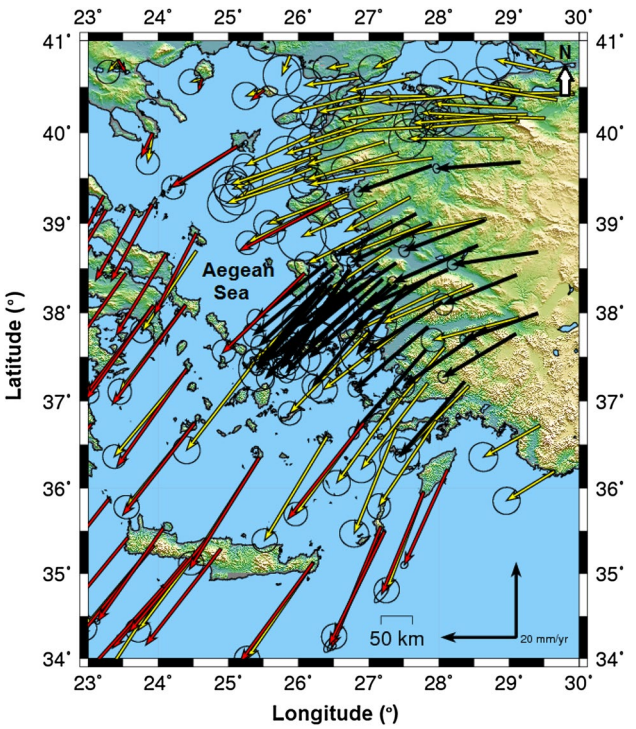


**Fig. 2** GPS velocities and their 95% confidence ellipses in a Eurasia-fixed reference frame (yellow vectors: McClusky et al. 2000; red vectors: Hollenstein et al. 2008, black vectors: Çırmık et al. 2017; Çırmık and Pamukçu 2017) (This figure is created by using Generic Mapping Tools (GMT); Wessel and Smith 1998)

Following this transformation, the plate-centric GPS velocities were inverted to estimate the angular velocities on the common sites velocities. Generally, in plate motion models, the motions of plates on the Earth's surface can be described by Euler rotations. In other words, the relative motions between any two plates can be described as a rotation about an Euler Pole (Euler theorem). Euler pole is the intersection of the rotation axis with the Earth's surface. Therefore, relative motions of plates can be defined by the rotations with the assumption of rigid plates on a spherical Earth (DeMets et al. 1990; Ahadov and Jin 2017; Stein and Wysession 2005). Application of Euler theorem in geophysics states that the displacement of one tectonic plate relative to other plates takes place as a rotation about the Euler pole of relative rotation between the plates (Goudarzi et al. 2014). In this study, calculation of Euler pole parameters (latitude, longitude, $\omega$) was performed using GPS linear velocity vectors. Then, the magnitude of linear velocity (v) on the station on Plate B, with respect to Plate A due to rotation around the North Pole, can be obtained using Eq. 1:

$$v = \omega_{AB} \cdot r \tag{1}$$

where $\omega$ is the magnitude (Euclidian length) of angular velocity (Euler plate rotation) vector and r is the position vector of the station of interest (DeMets et al. 1990). One can compute this vector cross-product by converting station latitudes and longitudes (and thus converting velocity vectors) either in global Cartesian coordinate system ($X$, $Y$, $Z$) or in local geodetic (north, east, up) system.

As a result, the estimated Euler pole parameters are given in Table 1, where $\omega_x$, $\omega_y$ and $\omega_x$ are called as the components of Euler vector and $\omega$ is called as the magnitude of the angular velocity calculated from Euler components.

It is seen from Table 1 that Gamit/Globk estimates of Euler parameters are smaller than their uncertainties, meaning that Euler pole in this study could be basically anywhere on Earth and it would not make a significant difference to the results of the velocity solution combination because the required rotation rate is so small (Floyd and Herring 2018). Differences at the common sites after the transformation are

given in Table 2 for Hollenstein et al. (2008) and Table 3 for McClusky et al. (2000).

## Determining the Complete spherical Bouguer (CSB) gravity anomaly

The satellite-based gravity models, Earth Gravity Model (EGM2008) (Pavlis et al. 2008), World Gravity Model (WGM2012) (Bonvalot et al. 2012), European Improved Gravity model of the Earth by New techniques (EIGEN6c-4) (Förste et al. 2014), Gravity field and steady-state Ocean Circulation Explorer (GOCE) and EGM2008 combined model (GECO) (Gilardoni et al. 2016) etc. have been used for decades. WGM2012 model is the first release of a high-resolution grid of the Earth's gravity anomalies (Bouguer, isostatic and surface free-air), calculated at global scale in spherical geometry by the Bureau Gravimétrique International (BGI) in the frame of collaborations with international organizations such as Commission for the Geological Map of the World (CGMW), UNESCO, International Association of Geodesy (IAG), International Union of Geodesy and Geophysics (IUGG), International Union of Geological Sciences (IUGS) and with various scientific institutions. WGM2012 gravity anomalies are derived from EGM2008 and DTU10 (Global Ocean Tide model of Technical University of Denmark) and include "1 × 1" resolution terrain corrections derived from ETOPO1 model (Bonvalot et al. 2012). The background removal that is based on Least Squares approximation was applied on CSB gravity anomaly to remove local anomalies or possible geological trend from data. In this step, WGM2012 model was used for the calculation of CSB gravity anomaly of Western Anatolia, Aegean Sea and Eastern Mediterranean. In this purpose, trend statistics of CSB gravity anomalies were calculated with the equations given in Table 4. The best fit between WGM2012 and trend statistic was the linear trend of CSB gravity anomaly (Fig. 3).

**Table 1** Euler pole parameters with respect to combined processing of Çırmık et al. (2017) and Çırmık and Pamukçu (2017) on Eurasia-fixed plate

| | $\omega_x \pm \sigma$ (°/Myr) | $\omega_y \pm \sigma$ (°/Myr) | $\omega_z \pm \sigma$ (°/Myr) | $\omega \pm \sigma$ (°/Myr) | Latitude (°N) | Longitude (°E) |
|---|---|---|---|---|---|---|
| Hollenstein et al. (2008) | −0.00061 ± 0.0303 | −0.01056 ± 0.0167 | −0.02564 ± 0.0307 | 0.0277 ± 0.046 | 67.58 | −93.31 |
| McClusky et al. (2000) | −0.00086 ± 0.02606 | −0.02035 ± 0.01519 | −0.03103 ± 0.03464 | 0.0389 ± 0.045 | 56.72 | −92.10 |

**Table 2** Differences at the common sites for Hollenstein et al. (2008)

| Station name | dN (mm) ± sN (mm) | dE (mm) ± sE (mm) | dU (mm) ± sU (mm) |
|---|---|---|---|
| KRPT | 8.08 ± 0.98 | −4.47 ± 0.84 | 0.99 ± 1.41 |
| BUCU | −1.78 ± 0.55 | 0.94 ± 0.47 | −0.00 ± 1.41 |
| GLSV | 0.17 ± 1.42 | 1.70 ± 1.11 | −0.00 ± 1.41 |
| ISTA | 1.08 ± 0.59 | −1.90 ± 0.52 | 0.00 ± 1.41 |
| MATE | −1.68 ± 0.55 | 0.69 ± 0.60 | −0.00 ± 1.41 |
| NICO | −1.40 ± 0.72 | 2.62 ± 0.59 | 0.00 ± 1.41 |
| TUBI | 2.02 ± 0.65 | −2.91 ± 0.57 | −0.00 ± 1.41 |
| WTZR | −0.45 ± 0.62 | 2.06 ± 0.75 | −0.00 ± 1.41 |
| ZECK | −0.25 ± 0.51 | 2.72 ± 0.79 | −0.00 ± 1.41 |

**Table 3** Differences at the common sites for McClusky et al. (2000)

| Station name | dN (mm) ± sN (mm) | dE (mm) ± sE (mm) | dU (mm) ± sU (mm) |
|---|---|---|---|
| KRPT | 5.71 ± 1.30 | −5.87 ± 1.43 | 0.99 ± 1.41 |
| WTZR | −2.44 ± 1.01 | 2.20 ± 1.09 | −0.00 ± 1.41 |
| NYAL | 0.53 ± 2.44 | −3.03 ± 2.04 | 0.00 ± 1.41 |
| KIT3 | −0.81 ± 1.91 | 2.26 ± 2.01 | −0.00 ± 1.41 |
| METS | −2.44 ± 1.95 | 1.51 ± 1.48 | −0.00 ± 1.41 |
| JOZE | −0.37 ± 1.11 | 0.62 ± 0.88 | 0.00 ± 1.41 |

**Table 4** Trend statistics of CSB gravity anomaly

| Model type | Formula | Model fit (%) |
|---|---|---|
| Linear | $m1+m2*x+m3*y$ | 42.2775 |
| Bilinear | $m1+m2*x+m3*y+m4*x*y$ | 41.2363 |
| 5th term | $m1+m2*x+m3*y+m4*x*y+m5*x*x$ | 39.1628 |
| 6th term | $m1+m2*x+m3*y+m4*x*y+m5*x*x+m6*y*y$ | 39.1345 |
| 7th term | $m1+m2*x+m3*y+m4*x*y+m5*x*x+m6*y*y+m7*x*x*x$ | 37.8922 |

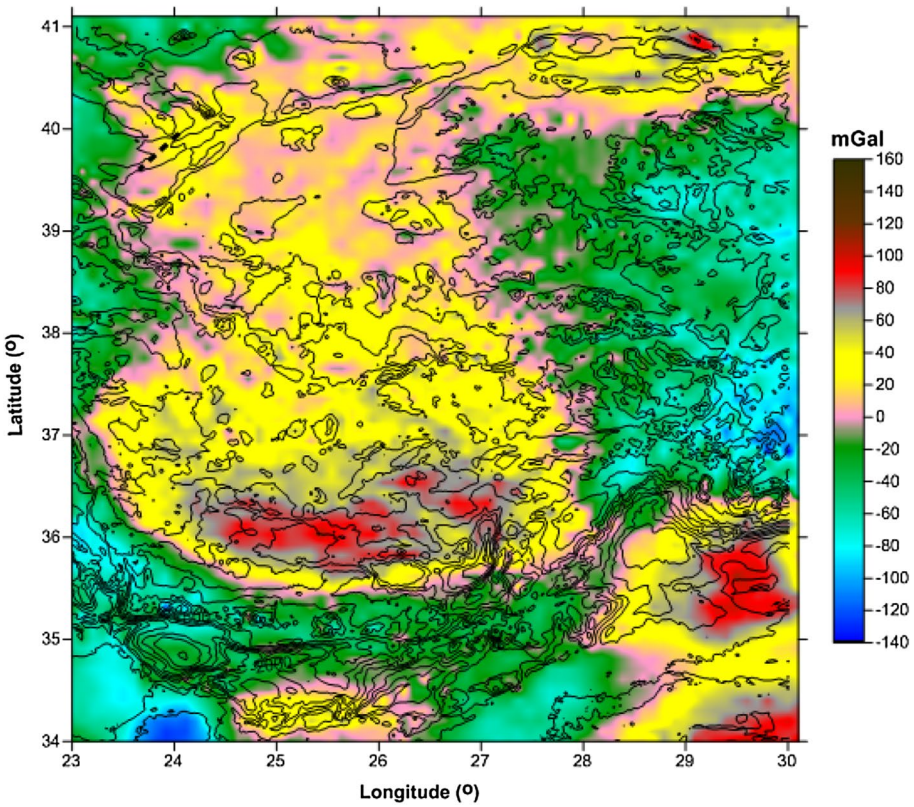


**Fig. 3** Linear trend removal map of WGM2012 gravity anomaly of the study area (The topographic data were obtained from TOPEX; Smith and Sandwell 1997)

## Discussion and conclusion

In this study, the study region was defined as seven microplates (Fig. 4) by combining the GPS velocities of previous studies (McClusky et al. 2000; Hollenstein et al. 2008; Çırmık et al. 2017; Çırmık and Pamukçu 2017). These microplates were separated in detail by taking into account the amplitudes and the directions of the GPS velocities by benefitting from the blocks proposed by Nyst and Thatcher (2004) for Izmir and its surroundings. Eurasia-fixed reference frame solutions of these studies were examined due to the amplitudes and the directions of GPS vectors. For examining the relation between the microplates, their boundaries and topography/bathymetry, the topographic and bathymetric map (ETOPO2; NOAA, N. 2006) of the study region was created (Fig. 5a). Therefore, due to the topographic and bathymetric differences (Fig. 5a), the study area was divided into three regions as regions A, B and C (Fig. 5b).

In Fig. 4, it is seen that the velocity vectors start to include the south component at the microplate No. 1. The movement mechanism of the microplate No.2 is exactly coherent with the tectonic escape model of McKenzie (1978). The microplate No. 3 does not move consistently with the movement mechanism of the westward tectonic escape model (McKenzie, 1978) with the effect of NAFZ mechanism. The topographic boundary between the microplate Nos. 2 and 3 (Fig. 5a, b) is the NAFZ, and NAFZ causes a boundary also at GPS velocity vector directions (Fig. 4). The microplate No. 4 is more stable with respect to Western Anatolia and Aegean Sea and moves like a different plate from the others. The movement mechanism of microplate No. 5, which is related with the movements

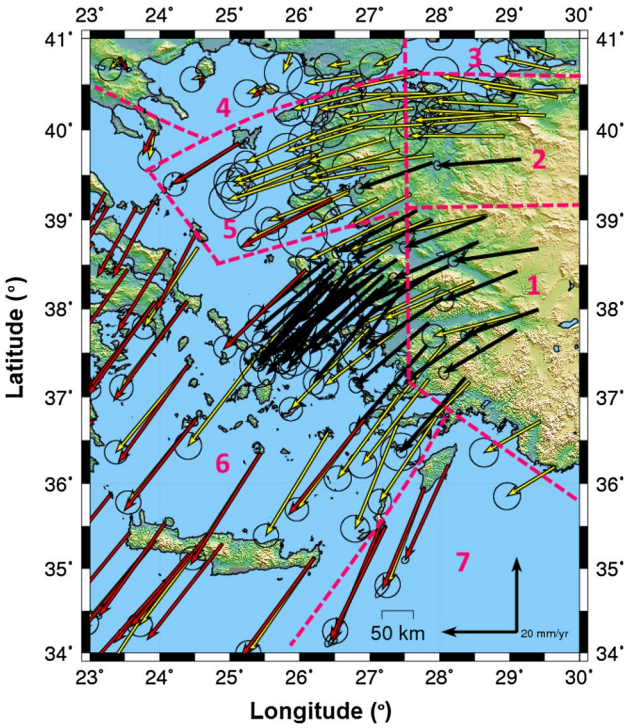


**Fig. 4** The views of the microplates created by the differences on the amplitudes and the directions of the GPS velocities given in Fig. 2

of microplate No. 2, gains south component in this area. Probably, the microplate No. 5, when come across a stable mechanism of microplate No. 4, is forced to rotate southward. The main boundary of microplate No. 5 can be seen clearly at the topography and bathymetry (Fig. 5a, b). The N–S trending boundary between the microplate Nos. 2 and 5 is also monitored clearly at the topography (Figs. 4, 5a, b).

The elongation of topographic structures is NE–SW trending in the region which locates at the westward of the N–S trending border (which locates at approximately between 27° and 28° longitudes) was called as region A in this study (Fig. 5b). This NE–SW trending topography of region A may be explained by encountering the movement of the body which comes from eastward with a stable plate and having south component velocity. The microplate No. 6 (Fig. 4) has velocity towards SW, but the south component is more dominant than other microplates and moves like a different plate. The region which locates north of Crete (Fig. 1) representing different bathymetries with respect to its surroundings was called as region C (Fig. 5b), and it includes the effect of the Hellenic Subduction zone. Additionally, it is seen clearly at GPS velocities (Fig. 4) that Hellenic Subduction zone composes a great effect between microplate Nos. 1 and 7. The directions of GPS velocities change approximately in 100 km between Anatolian plate and Rhodes Island (Fig. 4). Besides, the seismic activity (Fig. 6) is very high at microplate Nos. 1, 5 and 7 where the

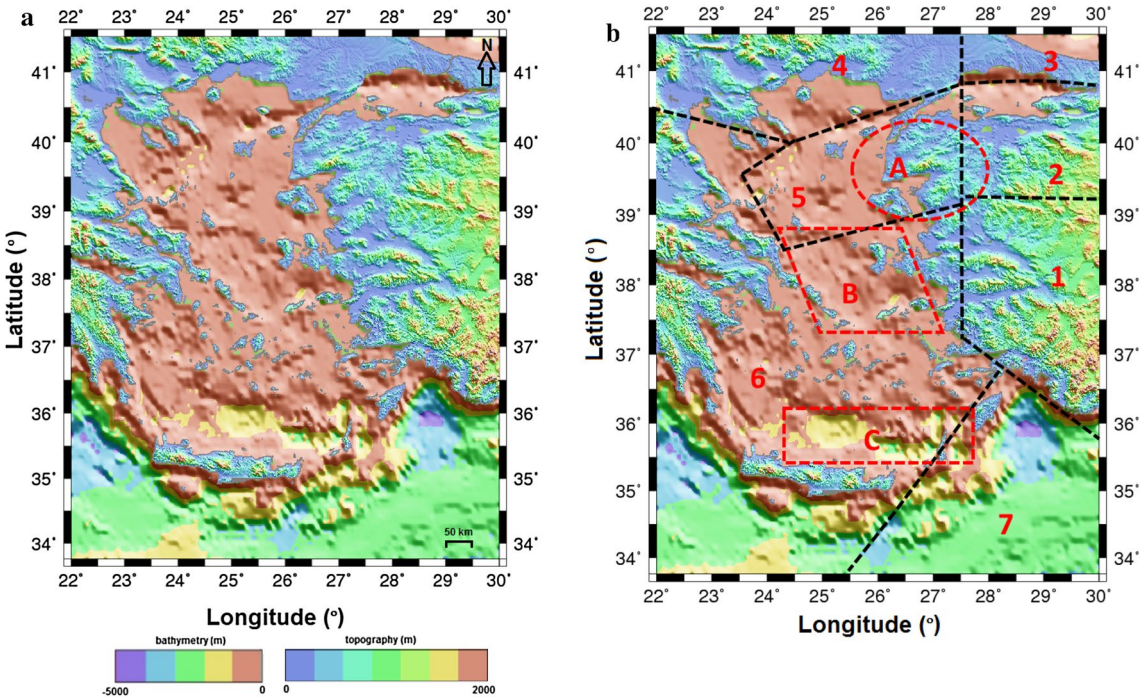


**Fig. 5** **a** The topographic and bathymetric map (ETOPO2; NOAA, N. 2006) of the study region. **b** The views of the microplates created by the differences on topography and bathymetry (**a**) related with the differences on the amplitudes and the directions of the GPS velocities given in Fig. 2. This figure is created by using Generic Mapping Tools (GMT) (Wessel and Smith 1998))

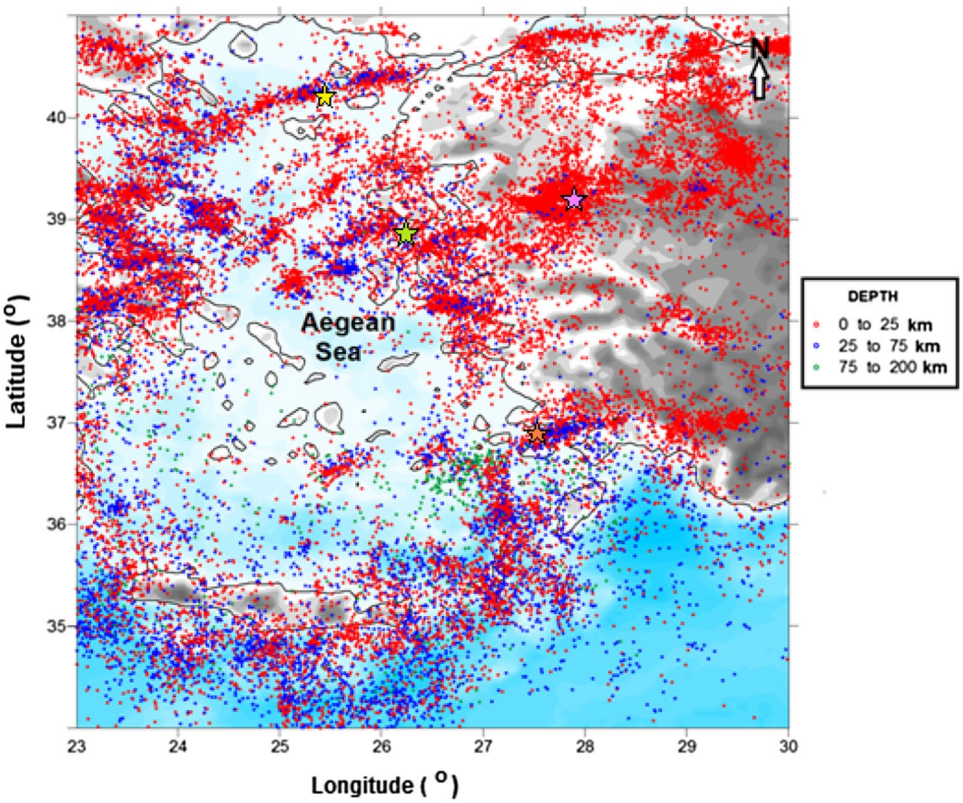


**Fig. 6** Topographic map of study area and the earthquake focal depth (km) distributions between the years 1973 and 2017 (from USGS). (Yellow star: Gokceada earthquake, $M_w = 6.5$; green star: Lesvos earthquake, $M_w = 6.2$; orange star: Gokova earthquake, $M_w = 6.5$; pink star = Manisa-Golmarmara earthquake, $M = 5.1$; AFAD) The topographic data were obtained from TOPEX; Smith and Sandwell (1997)

velocity directions and the transition of the mass movements change rapidly.

For interpreting the similarities between the seismicity and the microplate borders of GPS velocities, the earthquakes that occurred between the years 1973 and 2017, with magnitude ($M_w$) range between 2.5 and 9.0, were taken from US Geological Service (USGS) and the focal depth distribution map is shown in Fig. 6. For instance, the Gokceada earthquake (24 May 2014, $M_w = 6.5$; Republic of Turkey Prime Ministry Disaster and Emergency Management Authority (AFAD)) and Lesvos earthquake (12 June 2017, $M_w = 6.2$; (AFAD)) which occurred in microplate No. 5 (Fig. 4), Gokova earthquake (21 July 2017, $M_w = 6.5$; (AFAD)) which occurred in microplate No. 6 and Manisa-Golmarmara earthquake (27 May 2017, $M = 5.1$; (AFAD)) which occurred at the intersection of microplate Nos. 1, 2 and 5 represent the most seismically active structures of the region (Fig. 6) in the present.

In Fig. 6, the high seismicity represents the borders of the microplates, and also low and high seismicity transitions represent the border between the microplates (Fig. 4). For instance, the GPS vector directions and earthquake distributions of the microplate Nos. 6 and 7 present different characters. Additionally, the earthquakes appear in concentrated along the border between the microplate Nos. 4 and 5. While the borders obtained from GPS velocities (Fig. 4) and earthquakes distributions (Fig. 6) are evaluated together, it can be said that the intersection area of the microplate Nos. 1–2–5–6 represents high complex structure by noticing the high seismicity. Due to the obtained general views, the vertical motions are also effective in the region. It is known that the earthquakes occur at the plate boundaries in general. It is noticed from GNSS velocities (Fig. 4) that the mass movements are increasing and gaining south components while passing from microplate No. 1 to microplate No. 6. This case causes high deformation in microplate No. 6 as seen clearly in bathymetric changes (Fig. 5b) particularly in a region which was called as region B. Therefore, a new deformation zone (or zones) may be observed in that region in following geologic time scales with the effect of this high deformation.

In the study of Tirel et al. (2004), the regions between North Anatolian Trough and Cretan Sea (Fig. 1) were defined as "deformed areas" and "zones of recent thinning". The boundary between microplate Nos. 4 and 5 and region C are consistent with the regions which were defined as "zones of recent thinning" by Tirel et al. (2004). The directions of GPS velocities rotate to south, and the amplitudes of the velocities increase in the region located at the south of "zones of recent thinning" (Fig. 4) due to the slab retreat effect of Hellenic Subduction zone. This effect stops rapidly in the boundary between the microplate Nos. 1 and 7 (Fig. 4).

In the study of Bohnhoff et al. (2005) which was achieved with the focal mechanism results in Hellenic Subduction zone, it was explained that the plate boundary mechanism of Hellenic Arc included different angles. The boundary which has this angle differences coincides with the border between the microplate Nos. 6 and 7.

For evaluating the relationship between GPS velocities and the gravity values, the gravity anomalymap (Fig. 3) was divided into microplates (Fig. 7) due to the differences on the amplitudes of the gravity values. If Figs. 4 and 7 were evaluated together, it was determined that the boundaries of kinematic movements and the changes in the mass structures were almost same. Therefore, the directions of the GPS velocity vectors represent differences at the transitions between the tectonic elements which have low and high densities.

In the study region, the lowest amplitude gravity anomalies are seen in the Western Anatolia graben system and its southern part (Fig. 7). There is a transition zone between the longitudes 27° and 28° (Fig. 7) same as GPS velocities (Fig. 4) and earthquake focal depth distributions (Fig. 6). Besides, this transition zone between these longitudes was called as West Anatolia Transfer Zone (WATZ) by Gessner et al. (2013) and this zone was corrected by the Bouguer gravity anomaly study of Dogru et al. (2017). Besides, WATZ forms a boundary which separates west of Western Anatolia from Western Anatolian graben system. If the Bouguer gravity anomaly map (Fig. 7) is examined, the region containing the shear zone is characterized with negative gravity anomalies on graben system. The, respectively, lower amplitude gravity anomalies are related with the graben systems which contain high sediment thickness or the regions which have high heat flows (Dolmaz et al. 2005) and may be associated with the asthenospheric upwelling and rising temperature (Fig. 7). When Figs. 4, 5b, 6 and 7 were evaluated together, both the boundaries which were obtained from GPS velocities, bathymetry–topography and gravity, represent high seismic activities (Fig. 6) and this knowledge verifies that these boundaries are also the boundaries of the microplates.

In this study, unlike previous studies, the microplates which represented Western Anatolia were distinguished from each other in more detail by using the results of GPS study realized in and around Izmir (Çırmık et al. 2017). In the study of Çırmık et al. (2017), in addition to Eurasia-fixed-frame frame calculation, the GPS velocities were computed with respect to Anatolian-block fixed frame, and therefore, a boundary which separated the kinematic structure of Izmir from Western Anatolia graben tectonic structure was proposed. That boundary is consistent with the N–S directional border located between Western Anatolian microplate Nos. 1 and 6 (Fig. 4). The tectonic mechanism related with the microplate No. 7 (Fig. 4) is thought to be affected by the interplate geodynamic structure around Isparta angle (Fig. 1)

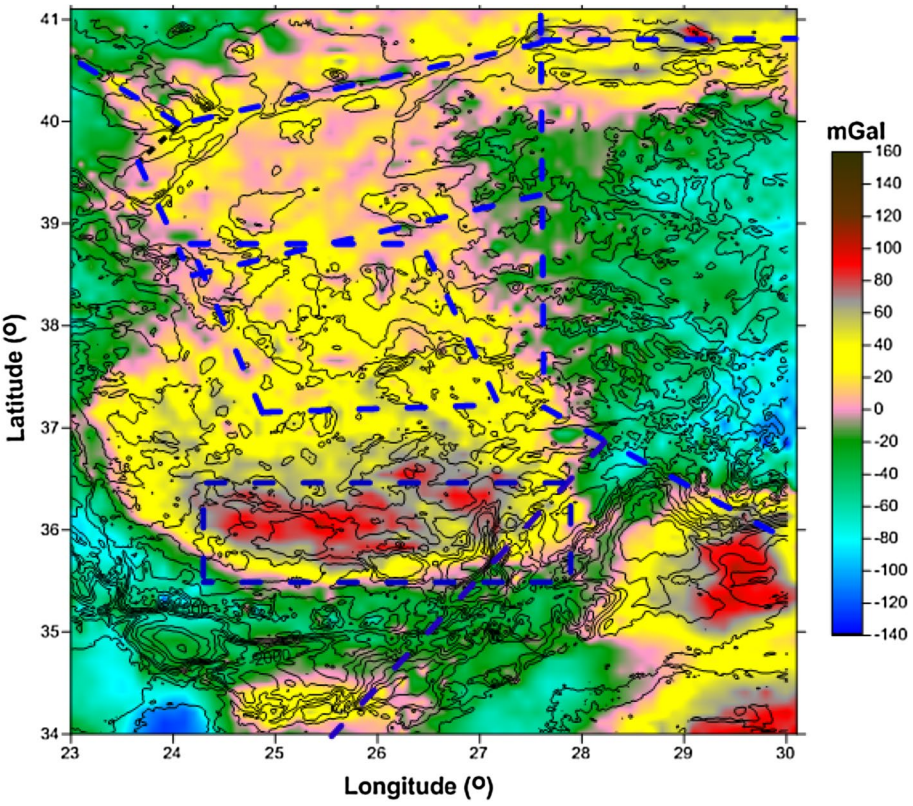


**Fig. 7** The views of the microplates created by the differences on the amplitudes of the gravity values given in Fig. 3

which was defined in the study of Över et al. (2016). Therefore, it is suggested that the continuity of Isparta angle where Mediterranean Sea, Aegean Sea and Western Anatolia intersect needs to be studied.

## References


Ahadov B, Jin S (2017) Present-day kinematics in the Eastern Mediterranean and Caucasus from dense GPS observations. Phys Earth Planet Int 268:54–64

Ambraseys N, Jackson JA (1990) Seismicity and associated strain of central Greece between 1890 and 1988. Geophys J Int 101(3):663–708

Armijo R, Meyer B, King G, Rigo A, Papanastassiou D (1996) Quaternary evolution of the Gulf of Corinth rift and its implications for the Late Cenozoic evolution of the Aegean. Geophys JR Astron 126:11–53

Bohnhoff M, Harjes HP, Meier T (2005) Deformation and stress regimes in the Hellenic subduction zone from focal mechanisms. J Seismo 9(3):341–366

Bonvalot S, Balmino G, Briais A, Kuhn M, Peyrefitte A, Vales N, Biancale R, Gabalda G, Reinquin F, Sarrailh M (2012) World gravity map. Commission for the Geological Map of the World. Eds. BGI-CGMW-CNES-IRD, Paris

Bozkurt E, Sözbilir H (2004) Geology of the Gediz Graben: newfield evidence and its tectonic significance. Geol Mag 141:63–79

Çırmık A, Pamukçu O (2017) Clarifying the interplate main tectonic elements of Western Anatolia, Turkey by using GNSS velocities and Bouguer gravity anomalies. J Asian Earth Sci 148:294–304

Çırmık A, Pamukçu O, Gönenç T, Kahveci M, Şalk M, Herring T (2017) Examination of the kinematic structures in Izmir (Western Anatolia) with repeated GPS observations (2009, 2010 and 2011). J African Earth Sci 126:1–12

DeMets C, Gordon RG, Argus DF, Stein S (1990) Current plate motions. Geophys J Int 101(2):425–478

Dewey JF (1988) Extensional collapse of orogens. Tectonics 7(6):1123–1139

Dewey JF, Şengör AMC (1979) Aegean and surrounding regions: complex multi-plate and continuum tectonics in a convergent zone. Geol Soc Am Bull 90(1):89–92

Dewey JF, Hempton MR, Kidd WSF, Şaroglu F, Şengör AMC (1986) Shortening of continental lithosphere: the neotectonics of eastern Anatolia-a young collision zone. In: Coward MP, Ries AC (eds) Collisional tectonics, vol 19. Geological Society of London, London, pp 3–36

Dogru F, Pamukçu O, Ozsoz I (2017) Application of tilt angle method to the Bouguer gravity data of Western Anatolia. Bull Miner Res Explor 155:45–55

Dolmaz MN, Hisarlı ZM, Ustaomer T, Orbay N (2005) Curie point depths based on spectrum analysis of aeromagnetic data, West Anatolian extensional province, Turkey. Pure Appl Geophys 162:571–590

Floyd M, Herring TA (2018) e-mail communications with Massachusetts Institute of Technology (MIT), Department of Earth Atmospheric and Planetary Sciences (EAPS)

Floyd MA, Billiris H, Paradissis D, Veis G, Avallone A, Briole P, McClusky S, Nocquet JM, Palamartchouk K, Parsons B, England PC (2010) A new velocity field for Greece: implications for the kinematics and dynamics of the Aegean. J Geophys Res 115:B10403

Förste C, Bruinsma SL, Abrikosov O, Lemoine JM, Marty JC, Flechtner F, Balmino G, Barthelmes F, Biancale R (2014) EIGEN-6C4 The latest combined global gravity field model including GOCE data up to degree and order 2190 of GFZ Potsdam and GRGS Toulouse. GFZ Data Serv 12:15. https://doi.org/10.5880/ICGEM.2015.1

Gessner K, Gallardo LA, Markwitz V, Ring U, Thomson SN (2013) What caused the denudation of the Menderes Massif: review of crustal evolution, lithosphere structure, and dynamic topography in southwest Turkey. Gondwana Res 24(1):243–274

Gilardoni M, Reguzzoni M, Sampietro D (2016) GECO: a global gravity model by locally combining GOCE data and EGM2008. Stud Geophys Geod 60:228–247

Goldsworthy M, Jackson J, Haines J (2002) The continuity of active fault systems in Greece. Geophys J Int 148(3):596–618

Goudarzi MA, Cocard M, Santerre R (2014) EPC: Matlab software to estimate Euler pole parameters. GPS Solut 18:153–162

Herring TA, King RW, Floyd MA, McClusky SC (2015) Introduction to GAMIT/GLOBK, Release 10.6. Massachusetts Institute of Technology, Cambridge

Hollenstein C, Müller MD, Geiger A, Kahle HG (2008) Crustal motion and deformation in Greece from a decade of GPS measurements, 1993–2003. Tectonophysics 449(1):17–40

https://www.afad.gov.tr/. Republic of Turkey Prime Ministry Disaster and Emergency Management Authority (AFAD)

Jackson J, McKenzie DP (1988) The relationship between plate motion and seismic moment tensors, and the rates of active deformation in the Mediterranean and Middle-East. Geophys J R Astron Soc 93:45–73

Kahle HG, Cocard M, Peter Y, Geiger A, Reilinger R, Barka A, Veis G (2000) GPS derived strain field within the boundary zone of the Eurasian, African, and Arabian plates. J Geophys Res 105(B10):23353–23370

Kahveci M, Pamukcu O, Cirmik AY, Gonenc T (2013) Using GPS data together with geophysical data: a case study from a seismically active region, Izmir. In: 6th international conference on recent advances in space technologies (RAST). IEEE, pp 231–236

Le Pichon X (1982) Land-locked oceanic basins and continental collision: eastern Mediterranean as a case example. In: Hsü K (ed) Mountain building processes. Academic, New York, pp 201–211

Le Pichon X, Angelier J (1979) The Hellenic arc and trench system: a key to the evolution of eastern Mediterranean area. Tectonophysics 60:1–42

Makris J (1978) The crust and upper mantle of the Aegean region from deep seismic soundings. Tectonophysics 46:269–284

Mart Y, Ryan WBF (2003) The tectonics of Cyprus Arc: a model of complex continental collision. Eur Geophys Soc Geophys Res Abstracts 5:02282

McClusky S et al (2000) Global Positioning System constraints on plate kinematics and dynamics in the eastern Mediterranean and Caucasus. J Geophys Res 105(B3):5695–5719

McKenzie DP (1972) Active tectonics of the Mediterranean region. Geophys J R Astron Soc 55:217–254

McKenzie DP (1978) Active tectonics of the Alpine-Himalayan belt: the Aegean sea and surrounding regions (tectonic of Aegean region). Geophys J R Astron Soc 55:217–254

Mercier JL, Sorel D, Vergely P (1989) Extensional tectonic regimes in the Aegean basins during the Cenozoic. Basin Res 2:49–71

NOAA, N (2006). 2-minute Gridded Global Relief Data (ETOPO2) v2

Nyst M, Thatcher W (2004) New constraints on the active tectonic deformation of the Aegean. J Geophys Res 109:B11406

Över S, Özden S, Kamacı Z, Yılmaz H, Ünlügenç UC, Pınar A (2016) Upper crust response to geodynamic processes beneath Isparta Angle, SW Turkey: revealed by CMT solutions of earthquakes. Tectonophysics 687:94–104

Pamukçu O (2016) Geodynamic assessment of Eastern Mediterranean region: a joint gravity and seismic b value approach. Arab J Geosci 9(5):1–13

Pamukçu O, Gönenç T, Çırmık YA, Kahveci M (2015) Investigation of the Sıgacık Bay's displacement characteristic by using GPS and gravity data in Western Anatolia. J Asian Earth Sci 99:72–84

Pavlis NK, Holmes SA, Kenyon SC, Factor JK (2008) An earth gravitational model to degree 2160: EGM2008. EGU Gen Assem 10:13–18

Reilinger R et al (2006) GPS constraints on continental deformation in the Africa, Arabia, Eurasia continental collision zone and implications for the dynamics of plate interactions. J Geophys Res 111:B05411

Reilinger R, McClusky S, Paradissis D, Ergintav S, Vernant P (2010) Geodetic constraints on the tectonic evolution of the Aegean region and strain accumulation along the Hellenic subduction zone. Tectonophysics 488:22–30

Seyitoğlu G, Scott BC (1991) Late Cenozoic crustal extension and basin formation in west Turkey. Geol Mag 128:155–216

Smith WHF, Sandwell DT (1997) Global seafloor topography from satellite altimetry and ship depth soundings. Science 277:1957–1962

Sorel D, Mercier JL, Keraudren B, Cushing M (1988) Le role de la traction de la Lithosphere Subducte Dans L'evolution Geodynamique Plio-Pleistocene De l'Arc Egeen: Mouvement Verticaux Alternes Et Variations Du Regime Tectonique. C R Geosci 307:1981–1986

Stein S, Wysession M (2005) An introduction to seismology, earthquakes, and earth structure. Blackwell Publishing, Oxford, pp 290–296

Taymaz T, Jackson J, Westaway R (1990) Earthquake mechanisms in the Hellenic Trench near Crete. Geophys J Int 102(3):695–731

Tirel C, Gueydan F, Tiberi C, Brun JP (2004) Aegean crustal thickness inferred from gravity inversion, Geodynamical implications. Earth Planet Sci Lett 228(3–4):267–280

Wessel P, Smith WHF (1998) New, improved version of the generic mapping tools released. Am Geosci Union 79:579

Yılmaz Y, Genç C, Gürer F, Bozcu M, Yılmaz K, Karacık Z, Altunkaynak Ş, Elmas A (2000) When did the western Anatolian grabens begin to develop? In: Bozkurt E, Winchester JA, Piper JDA (eds) Tectonics and magmatism in Turkey and surrounding area, vol 173. Geological Society of London, London, pp 353–384



View publication stats